Dynamical behavior of a pacemaker neuron model with fixed delay stimulation

Leonel Gómez,[1,2] Ruben Budelli,[1] and Khashayar Pakdaman[3]
[1]*Sección Biomatemática, Facultad de Ciencias, Universidad de la República, Iguá 4225, Montevideo 11400, Uruguay*
[2]*Laboratoire Dynamique des Processus Sensoriels, Institut Alfred Fessard, CNRS, 91190 Gif-sur-Yvette, France*
[3]*Inserm U 444, Faculté de Médecine Saint-Antoine, 75251 Paris, France*
(Received 23 March 2001; revised manuscript received 6 September 2001; published 26 November 2001)

In physiological and pathological conditions, many biological oscillators, such as pacemaker cells, operate under the influence of feedbacks. Fixed delay stimulation is a standard preparation to evaluate the effects of such influences. Through the study of the Hodgkin-Huxley model, we show that such recurrent excitation can lead to regular and irregular discharge trains with interdischarge intervals that are up to several multiples of the period of the oscillator. In other words, we show that recurrent excitation can considerably slow down the firings of the pacemaker. This result contrasts with previous studies of similar preparations that have reported that fixed delay stimulation leads to a bursting pattern in which regimes of high-frequency firing alternate with periods of quiescence. We elucidate the mechanisms underlying the behavior of the oscillator under fixed delay perturbation through the analysis of the dynamics of a well-known two-dimensional oscillator, namely, the Poincaré oscillator.

DOI: 10.1103/PhysRevE.64.061910 PACS number(s): 87.10.+e, 07.05.Mh

I. INTRODUCTION

Fixed delay stimulation has been used as an experimental protocol for the analysis of a variety of biological systems, such as neurons, the respiratory system, heart-cell aggregates, and electric fish [1–4]. This methodology involves stimulating the system, say a pacemaker neuron, at a fixed time following each discharge. Thus fixed delay stimulation is the most elementary preparation for the study of the influence of recurrent loops. Such preparations model self-connections, such as autapses [5,6], or more complex feedback paths including several intermediate stages that occur widely in biological systems such as neuronal assemblies.

Many experimental and theoretical studies on fixed delay stimulation in oscillating systems, such as pacemaker cells or heart-cell aggregates have shown that such feedback can lead to bursting, that is, a repetitive succession of high-frequency discharges separated by long quiescent intervals [1,2,7,8]. The general mechanism underlying this form of response is well understood [8]. Namely, within a burst, each discharge is elicited by the stimulation following the previous firing after the fixed delay. So that the interdischarge intervals inside the burst are close to the delay. The excitability of the membrane decreases progressively during this stage of high activity. This process is referred to as threshold fatigue. The buildup of fatigue is responsible for stopping the burst. The process starts anew once the system recovers its excitability. The biophysical mechanisms underlying threshold fatigue varies from one preparation to another. For instance, in heart-cell aggregates, threshold fatigue is due to the accumulation of intracellular sodium ions during the burst [2].

In the present work, we show that, under fixed delay stimulation, a wide class of oscillators display some forms of behavior that are drastically different from those mentioned above. This new form of discharge, in contrast with the bursting pattern, is characterized by the fact that recurrent excitation, rather than accelerating the firing, considerably slows it down, with interdischarge intervals that can be several times longer than the period of the unperturbed oscillator. We illustrate this paradoxical slowing down of the pacemaker through recurrent excitation in the Hodgkin-Huxley (HH) neuron model, which is a generic model for excitable and oscillating membranes [9]. The mechanisms underlying this phenomenon are elucidated through the analysis of the response of a two-dimensional oscillator to fixed delay stimulation.

This paper is organized as follows. The slowing down effect of recurrent excitation is presented in Sec. II. The mechanisms underlying this phenomenon are analyzed in Sec. III. Finally, the results are discussed in Sec. IV.

II. EFFECT OF RECURRENT EXCITATION

We first illustrate the slowing down induced by the recurrent excitation with a compartmental HH oscillator. This model is succinctly described below. The details are given in the Appendix and in Table I.

The compartmental HH model is constituted by an active soma and an active axon. The soma is stimulated by a constant current I. The end tip of the axon is connected to the soma through an excitatory synapse so that the neuron is self-exciting (upper panel of Fig. 1). Each action potential, when reaching the end tip of the axon, evokes a postsynaptic current in the soma. The delay (d) is the time elapsed between the discharge of a spike in the soma and the start of the postsynaptic current. The maximal synaptic conductance, denoted by G_{max} represents the strength of the recurrent connection.

In the absence of recurrent excitation, i.e., $G_{max}=0$, the system stabilizes in a periodic firing of period $N=24.94$ ms referred to as the natural firing period [top panel in Fig. 1(b)]. Time variables will be expressed either in milliseconds (ms) or as normalized values (in relation to N). Depending on the value of the delay and the synaptic strength G_{max} (maximal conductance), the recurrent connection can have drastically different effects on the firing of the model. In some instances, the feedback accelerates the firing, as expected in the case of recurrent excitation. That is, the

TABLE I. HH model parameters.

Symbol	Value	Definition
C	1 μF/cm^2	Membrane capacitance
G_{Na}	0.12 ohm^{-1}/cm^2	Sodium conductance
E_{Na}	50 mV	Sodium equilibrium potential
G_K	0.036 ohm^{-1}/cm^2	Potassium conductance
E_K	-77 mV	Potassium equilibrium potential
G_l	0.0003 ohm^{-1}/cm^2	Leak current conductance
E_l	-54.3 mV	Leak current equilibrium potential
E_{epsp}	0 mV	Excitatory postsynaptic potential (EPSP) reversal potential
T_e	6.3 °C	Temperature
r_a	35.4 Ωcm	Axial resistance
τ	2 ms	EPSP time constant
D_{soma}	30 μm	Soma diameter
D_{axon}	2 μm	Axon diameter
L_{axon}	50 μm	Axon long
I	0.5 nA	Injected current

model fires with a period slightly longer than the delay, corresponding to the time it takes for the postsynaptic potential evoked back by each discharge to induce an action potential [middle panel in Fig. 1(b)]. In others, the interdischarge intervals take on values that are several times longer than the natural period, and their succession can be regular or irregular. This is illustrated in the bottom panel in Fig. 1(b), where for a delay of 0.433, the interdischarge intervals range from 61.44 to 97.6 ms, that is almost four times the natural period. It is in these situations that the fixed delay stimulation considerably slows down the firing of the pacemaker.

The upper panel in Fig. 2 shows the dependence of this phenomenon on the delay, and the lower one shows its dependence on both the delay and the synaptic strength. In the former, referred to as the interspike interval diagram (ISID), the values of the interspike intervals occurring during the stationary regime are represented against the delay. For example, if for a given delay value, the model stabilizes into a periodic firing with a period close to N, then the stationary interspike interval for this delay is indicated by a point with ordinate close to one. If for another delay d, it stabilizes in a period-three pattern, three points appear in the vertical line by d. The ISID is thus similar to a bifurcation diagram displaying the orbits of the stationary regimes of the system that appear for different values of the parameter d.

The ISID is constituted by several qualitatively distinct regions, corresponding to different firing regimes. For both short and long delays, it is constituted by a single line indicating that the unit fires periodically with a period close to the natural one. It is in the intermediate range of delays, where the ISID takes on a christmas-tree-like shape, that the strong slowing down takes place. In this parameter range, the ISID displays discontinuities between interspike intervals that are up to four times longer than the natural firing period. In this regime, the discharge pattern of the neuron can be periodic or more complex, as suggested by the fact that for some values of the delay, there is more than one interspike interval in the ISID. These multiple intervals represent either periodic firings with a repetition of several interspike intervals, or aperiodic behavior.

The above descriptions were concerned with the dependence of the slowing on the delay, for a given value of the feedback strength. The lower panel in Fig. 2 completes these by showing how the maximal interspike interval varies when both the delay and the self-connection strength are modified. The surface spirals up around a central peak. The lower regions represent the regimes where the model fires rapidly, whereas the peak and the neighboring range are those where the slowing down occurs. Cuts of this three-dimensional representation made at constant G_{max} display the christmas-tree-like shape such as the one shown in the upper panel of Fig. 2.

The remainder of this paper is devoted to the analysis of the mechanisms underlying the slowing down of the firing and its dependence on the delay and the connection strength.

III. ANALYSIS

First, we show that a low-dimensional oscillator with threshold can reproduce the behavior of compartmental pacemaker model depicted in the previous section. Then using this model, we analyze the changes occurring in the response of the model with delayed feedback in terms of geometrical properties of one-dimensional return maps.

More precisely, we consider the Poincaré oscillator (PO) with threshold undergoing fixed delay stimulation. The standard PO and its variants have been widely used in the analysis of forced biological oscillators [10]. The PO is described by the following equations in polar coordinates (ρ, ϕ):

$$\frac{d\rho}{dt} = K\rho(1-\rho),$$

$$\frac{d\phi}{dt} = 1. \tag{1}$$

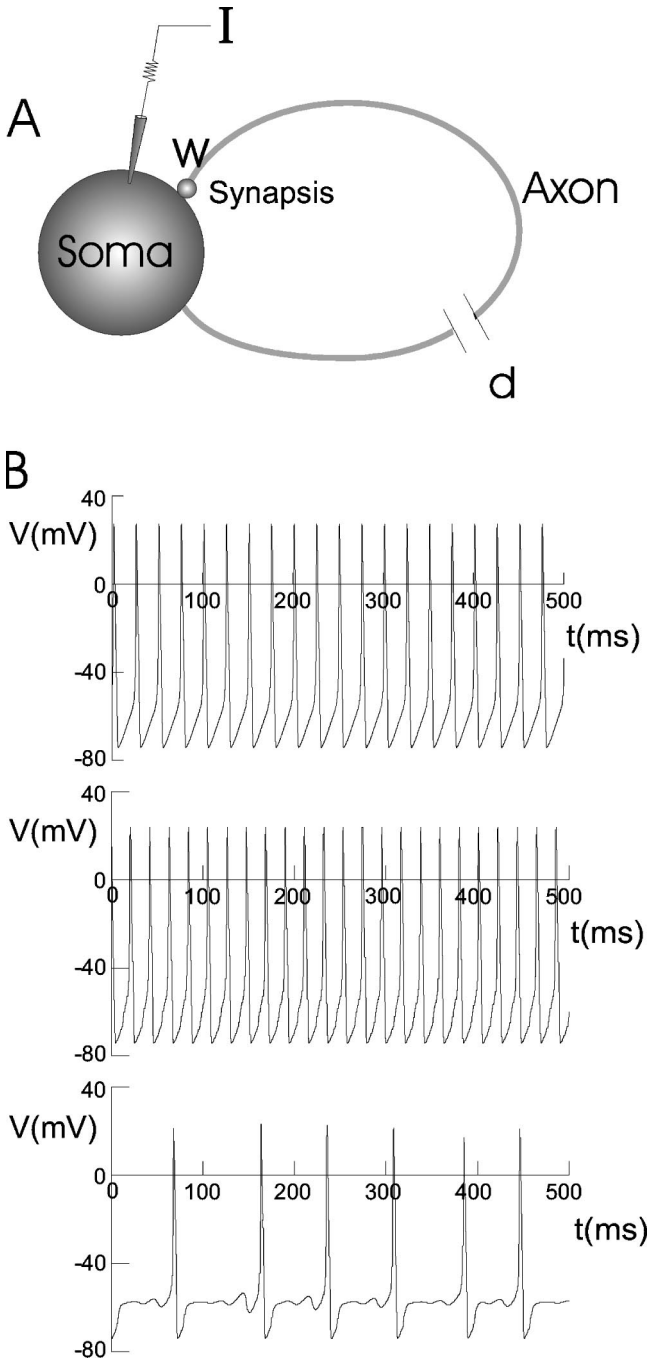

FIG. 1. (a) A neuron with recurrent excitatory connection of strength G_{max} and transmission delay d is represented. The neuron receives a constant input current I. (b) *Time course of the membrane potential for the* HH *model*. Upper panel shows the control discharge, i.e., $G_{max}=0$. The next two graphs are examples with recurrent excitation $G_{max}>0$ and normalized delays: 0.521 and 0.433, respectively. Horizontal axis: time in milliseconds, Vertical axis: voltage in mV.

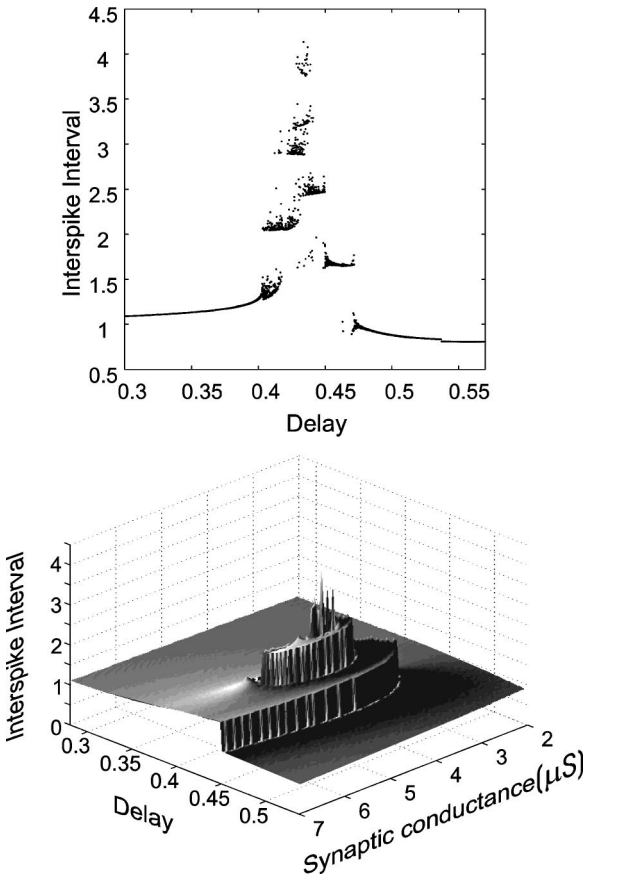

FIG. 2. *Upper panel*: Interspike intervals for different delays of the HH neuron model with delayed recurrent excitation are represented as a function of the delay. Vertical axis: interspike intervals normalized by the natural period; horizontal axis: delay normalized by the natural period. *Lower panel*: Maximum interspike interval as a function of the delay and the amplitude of the EPSP from the HH model.

The PO displays an unstable equilibrium point at the origin, and a stable limit cycle (the unit circle $\rho=1$). In the phase space, trajectories of all initial conditions, except the equilibrium point, wind counterclockwise around the origin and tend to the limit cycle. Perturbations are modeled as horizontal impulses of amplitude a that drive the system from its position $\overline{X}=(x,y)$ to the point $\overline{X}+\overline{a}=(x+a,y)$.

In the standard PO, the passage of the system through $\phi=0$ is taken as the reference event, or in other words the firing. However, in the present work, we assume that the PO also possesses a threshold in the sense that this model generates a spike only when the variable $x(t)=\rho(t)\cos\phi(t)$ is larger than a value ρ_T with $0<\rho_T<1$ when the state of the system crosses the $\phi=0$ line [11]. We refer to this oscillator as the PO with threshold. The inclusion of the threshold in the model is motivated by two observations: (i) the standard PO undergoing fixed delay stimulation, while generating complex dynamics, does not exhibit slowing down of the firing larger than half a period [3], so that this model needs to be modified in order to capture the behavior of the compartmental model, and (ii) the discontinuities in the ISID of the compartmental model that are responsible for the slowing down show that parameter values close to each other can lead the system to produce interspike intervals that differ in an amount close to the natural period. This form of behavior results from the existence of an event surface in the phase space that separates trajectories leading to a discharge from

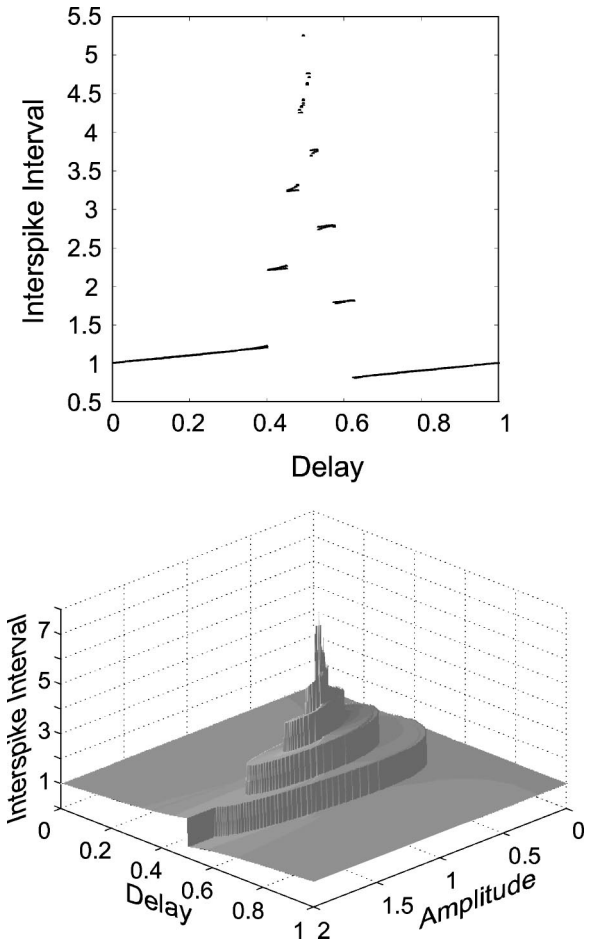

FIG. 3. *Upper panel*: The steady state interspike intervals of the Poincaré oscillator with delayed recurrent excitation are represented as a function of the delay. Vertical axis: interspike intervals normalized by the natural period; horizontal axis: delay normalized by the natural period. *Lower panel*: Maximum interspike interval as a function of the delay and the amplitude of the PO model.

those that do not [12]. The event surface is itself a consequence of the firing threshold, thereby motivating the inclusion of this feature in the PO.

The panels in Fig. 3 that represent the ISID of the PO with threshold undergoing fixed delay stimulation, and the dependence of the largest interspike interval of this model on the feedback delay and strength clearly show that the response of this model displays strong similarities with that of the compartmental model (compare with Fig. 2). In the ISID of the PO with threshold, one observes the same christmas-tree-like form at intermediate delays as for the compartmental model, and for both models, in the two-parameter diagrams, the surface representing the largest interspike interval spirals around a central peak-shaped region. This similarity reveals that the PO with threshold contains the key ingredients leading to the slowing down of the firing due to fixed delay stimulation. In the remainder of this section, we take advantage of this to clarify the mechanisms underlying this phenomenon through the construction of Poincaré return maps describing successive piercing of an appropriate surface by a trajectory. We first describe the construction of this

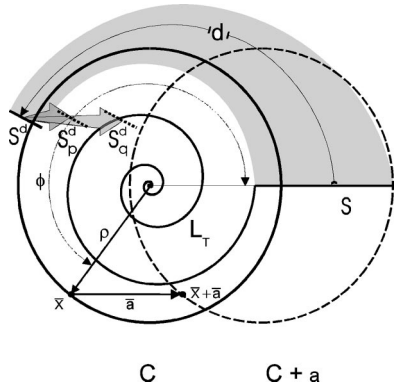

FIG. 4. *PO phase space*: The system has a stable limit cycle $\rho=1$, represented by the circle, and an unstable equilibrium point at the origin. A spike is generated when the system goes through the phase 0, with a radius larger than $\rho_T=0.8$ (the event surface S). The spiral (L_T) represents the trajectory leading to the threshold (the edge of the event surface). The solid circle C is limit cycle $\rho=1$, the dashed circle $C+a$ is the locus of the points on the limit cycle after a perturbation of amplitude a. S^d represents the position of the points in S after a delay d has elapsed. S_q^d and S_p^d are the translations of S^d by the synaptic action for two different values of a.

map for the PO with threshold, and use it as a basis for that of the compartmental model.

For the PO we consider the return map associated with the Poincaré section defining the firing, i.e., $\phi=0$ and $\rho \in (\rho_T, 1+a)$. Depending on the delay and stimulation strength, these maps take on various forms, resulting from the diverse dynamics of the model. The construction of the maps clarifies the relation between, on the one hand, the delay, the stimulation strength and the firing threshold and, on the other hand, the geometrical characteristics of the map. We illustrate this point through representative examples.

In the phase space of the PO, we denote by L_T the event surface, which is the backwards trajectory of the threshold $[(\rho,\phi)=(\rho_T,0)]$, i.e., the backwards trajectory of $\phi=0$ and $\rho=\rho_T$. The line L_T goes from the threshold to the origin spiraling around it. It is the relative position of this line with respect to that of the points after the delivery of the stimulation that determines the shape of the return map. More precisely, the construction of the return map is done according to the following steps (Fig. 4). First, points on the Poincaré section, denoted by S [$\phi=0$, $\rho \in (\rho_T, 1+a)$ in figure], move along their trajectory for a time equal to the delay d (their locus is S^d in Fig. 4). At this time, they are translated by an amount a due to the stimulation delivery. Two examples of such loci for parameters p and q are denoted by S_p^d and S_q^d in Fig. 4. From this stage on, the points move along their trajectories until they hit S at some time. It is the relative position of S^d with respect to L_T that determines the key characteristics of the return map.

For delays and amplitude ranges where S_a^d does not intersect L_T, such as for p, all points on S_p^d reach S in less than a cycle. The resulting Poincaré map is a continuous contraction, intersecting the diagonal in a single point. This stable fixed point of the map represents the unique intersection of a

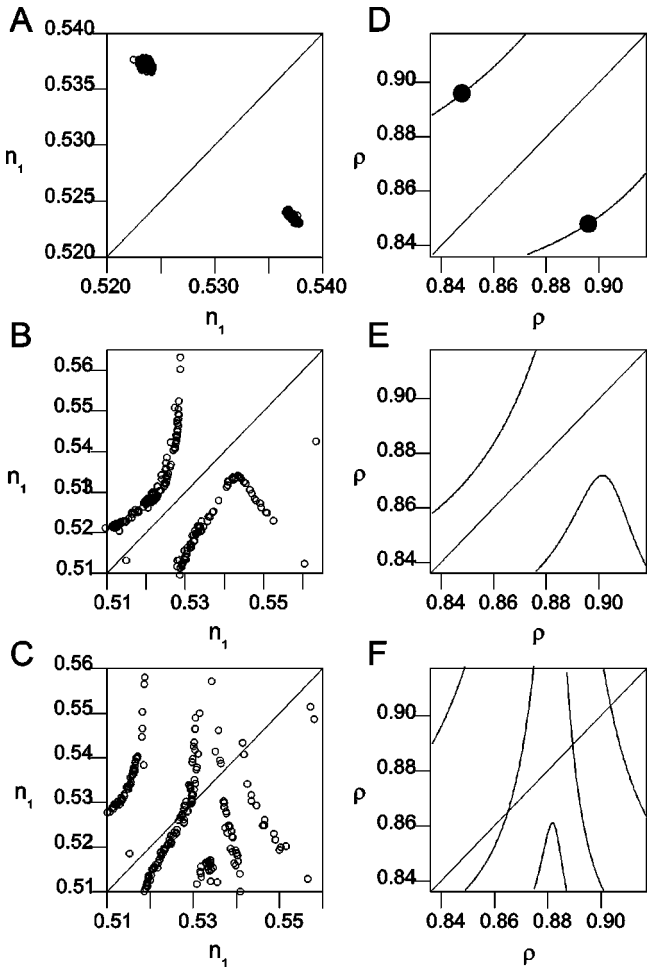

FIG. 5. *Return maps*. Left: The value of n, when the membrane potential reaches zero from negative values as a function of the previous one, for different stimulation parameters. (a) $G_{max}=0.004\,76$, $d=0.43$; (b) $G_{max}=0.004\,18$, $d=0.43$; (c) $G_{max}=0.0046$, $d=0.43$. Right: ρ when $\phi=0$ as a function of the previous one, for different stimulation parameters, (d) $d=0.495$, $a=0.84$, black circles correspond to period 2 stable orbit; (e) $d=0.497$, $a=0.935$; (f) $d=0.499$, $a=0.965$.

stable periodic orbit with the Poincaré section.

When S_a^d and L_T intersect at exactly one point (e.g., S_q^d in Fig. 4), the return map has a single discontinuity and presents a stable orbit with period 1 or 2 [e.g., Fig. 5(d)]. In fact, as the number of intersection points between S_a^d and L_T increases, the behavior of the model becomes more complex [e.g., Fig. 5(e)]. More precisely, when S_a^d cuts many times different turns of L_T, the return map presents segments with its image covering several times the same portion of the same interval of S [e.g., Fig. 5(f)]. Furthermore, when S_a^d cuts many turns of L_T and some of them twice, the return map presents a relative maximum [e.g., Fig. 5(f)]. It is these two types of maps that can exhibit complex behavior, including chaos. Typically this situation occurs when d corresponds to a value of ϕ close to 0.5 and a is close to one. This analysis is in complete agreement with the numerical results shown in Fig. 3 and successfully accounts for the various behavior of the model and their dependence on the delay and the feedback strength.

The previous analysis clarified how complex behavior of the PO with threshold arise thanks to the construction of return maps. This analysis guides also that of the compartmental HH model. The construction of a section for this model is more arduous, since even the system without feedback is 84 dimensional, requiring the definition of an 83-dimensional section in the phase space. The addition of recurrent excitation makes the problem more complex, because perturbations are not delivered as impulses, but rather as synaptic currents. Therefore, instead of defining a section based on the phase portrait of the system, we construct it along the same line as for the PO: we consider that whenever the system generates a spike at the level of the soma, it crosses the section. Inspired by the similarity between this model and the PO, we plot the return map of the projection on a one dimension of the system at this point (we take n_1). The left column in Fig. 5 shows this map for different values of the amplitude. Results on Fig. 5(a) exhibits two fixed points, corresponding to a period two repetitive firing. Figures 5(b) and 5(c) show results corresponding to a high-order periodicity or chaos. The points on the HH Poincaré maps present a ''noiselike'' dispersion due to the fact that the full Poincaré map is 83 dimensional and the influence of the other variables has been omitted. Nevertheless, the return maps of the HH model display striking similarity with those of the PO thereby further supporting our claim that similar mechanisms underlie the slowing down of firing caused by self-excitation in both models.

IV. DISCUSSION AND CONCLUSION

Many biological systems operate under the influence of feedback mechanisms. For neuronal systems, this feedback can take the form of recurrent excitation, i.e., when the discharge of a neuron, after possibly going through several interconnections can activate back an excitatory response in the same neuron. Such processes can have functional roles for (i) amplifying activity in neuronal assemblies, (ii) reverberating the activity and leading to some form of memory or (iii) generating rhythmic patterns such as in central pattern generators.

The self-exciting neuron, i.e., the neuron undergoing fixed delay stimulation, is considered as both the experimental and theoretical system that can reveal the influence of feedbacks on neuronal behavior [1,7,8,13,14]. Previous studies of fixed delay perturbation of neuronal pacemakers had produced bursting patterns composed of phases of active firing alternating with regimes of quiescence [1,8]. In contrast, our work revealed a behavior in comparison with these, namely, that recurrent excitation can also considerably slow down neuronal firing.

Our purpose was the elucidation of the mechanisms underlying recurrent excitation induced slowing down. The results presented in Sec. III shows that the PO with threshold reproduces well the dynamics of the HH model and clarified the mechanisms underlying this behavior. The key ingredient for the slowing down is the combination of two factors: one that the system displays a threshold, and second that the perturbations take the system to the vicinity of an unstable

equilibrium point. The qualitative comparison is satisfactory since it leads to a heuristic explanation of the behavior of the HH model in the presence of recurrent excitation.

The analysis also shows that complex behavior results from expansions taking place near the unstable equilibrium point (where nearby trajectories tend to diverge exponentially), leading to steeper return maps. The combination of this expansion and the discontinuities (producing many-to-one maps) may lead to sensitivity to initial conditions, the hallmark for complex behavior. The simplicity of these factors suggests that similar behavior can be expected in a wider class of systems.

Finally, one issue of importance is the origin of the difference between the slowing down reported in this work and the bursting patterns observed in previous studies. The interplay between two factors, namely, the stimulation characteristics, i.e., the delay and the stimulus amplitude, and the intrinsic properties of the oscillator account for this difference. This is discussed in the following.

One source of difference resides in the stimulus characteristic associated with each of the two types of behavior. More precisely, given a delay value, for bursting to occur it is only necessary that the stimulus amplitude be large enough to evoke an action potential if it is applied after a delay time following a discharge. This condition does not impose severe restrictions on the ranges of potential of delays and amplitudes susceptible to evoke bursting. In contrast, slowing down is possible only for the restricted ranges of delays and amplitudes that take the system to the vicinity of the unstable equilibrium point. Figure 2 shows that this range corresponds to the specific region where there is a sand-castle-like structure. This difference between the parameter ranges corresponding to each of the behaviors could be one reason why slowing down was not observed in some of the previous studies. Indeed, in most of these, the stimulus amplitudes were large and may have been far from the range that could potentially lead to slowing down of the firing.

The second important difference comes from the intrinsic properties of the oscillators. As mentioned previously, the key factor responsible for bursting is threshold fatigue, i.e., the progressive decrease of membrane excitability during sustained firing. To display bursting in response to fixed delay stimulation, the process responsible for threshold fatigue must have a time scale longer than the delay so that fatigue can accumulate during successive firings and eventually halt the discharges. In other words, whether bursting is observed or not depends on the relation between an intrinsic time scale of the oscillator and the delay. In the model considered in this work, the time scale of fatigue is short. Thus, even when the stimulus characteristics satisfy the necessary conditions for bursting mentioned in the previous paragraph, fatigue does not build up during successive firing, and the model fires unceasingly with a period close to the delay.

In conclusion, bursting and slowing down are two possible behaviors in the presence of excitatory feedback loops. The conditions for their occurrence depend both on the stimulus characteristics and the intrinsic characteristics of the oscillators. In general, fixed delay stimulation with a large stimulus amplitude of a system with a slow threshold fatigue recovery would lead to bursting, while, in oscillators with a rapid recovery, delays and stimulus amplitudes that take the system within the neighborhood of an unstable equilibrium point would slow down the system's firing.

ACKNOWLEDGMENTS

L.G. and R.B. were partially supported by CEE International Cooperation Contract No. CI1*CT92 0085 and cooperation program ECOS sud (France-Uruguay).

APPENDIX: THE MODEL PARAMETERS

The soma is modeled as a single spherical compartment and the axon as 20 cylindrical compartments. The dynamics of the compartments are governed by the following set of differential equations:

$$C_j \frac{dV_j}{dt} = G_{Na}^j m_j^3 h_j (E_{Na} - V_j) + G_K^j n_j^4 (E_K - V_j) + G_l^j (E_l - V_j) + I_j ,$$

$$I_1 = g_{1,2}(V_2 - V_1) + I_{epsp} + I_{stim} ,$$

$$I_j = g_{j-1,j}(V_{j-1} - V_j) + g_{j,j+1}(V_{j+1} - V_j) \quad \text{if} \quad 1 < j < 21,$$

$$I_{21} = g_{20,21}(V_{20} - V_{21}),$$

$$I_{epsp} = (E_{epsp} - V_1) g_{epsp}(t - d - T),$$

$$I_{stim} = I,$$

$$\frac{dm_j}{dt} = \frac{m_\infty(V_j) - m_j}{\tau_m(V_j)},$$

$$\frac{dh_j}{dt} = \frac{h_\infty(V_j) - h_j}{\tau_h(V_j)},$$

$$\frac{dn_j}{dt} = \frac{n_\infty(V_j) - n_j}{\tau_n(V_j)}.$$

The index j indicates the compartment number, $j=1$ being the soma, $1<j<21$ the intermediate compartments of the axon and $j=21$ the end tip of the axon. Compartment 1 is connected only to compartment 2, and 21 only to 20, others are connected to the two adjacent ones. C_j is the membrane capacitance at compartment j. G_{Na}^j, G_K^j, and G_l^j are the maximum conductances for the sodium, potassium, and leak currents for compartment j, respectively. E_{Na}, E_K, and E_l are the reversal potentials for the sodium, potassium, and leak currents, respectively. For each compartment, V_j is the membrane potential, m_j and h_j the sodium current activation and inactivation variables, respectively, and n_j the potassium current activation variable. The input current I_j is the summation of the currents received from the adjacent compartments plus, possibly constant and synaptic currents for the soma. T represents the last time the model fired a spike defined as V_{21} increasing beyond $V_t = 0$ mV.

The synaptic current is defined as $I_{epsp}=g_{epsp}(t-T)(V-E_{epsp})$, where the synaptic conductance is given by an alpha function:

$$g_{epsp}(t-T)=0 \quad \text{for } t<T,$$

$$g_{epsp}(t-T)=G_{max}\frac{(t-T)}{\tau}\exp\frac{-(t-T-\tau)}{\tau} \quad \text{for } t>T, \tag{A1}$$

where $T=t_{spike}+d$, with t_{spike} the spike arrival time, G_{max} is the maximal synaptic conductance, τ is the characteristic synaptic time scale, i.e., the synaptic conductance is negligible when $t-T>5\tau$.

The simulations were carried out using the V3.1 Neuron simulator [15] running on a Sun Sparkstation 5, using a time step of 0.01 ms. Smaller time steps did not affect the results.

In order to mimic a pacemaker neuron, the model is stimulated by a constant depolarizing current ($I=0.5$ nA) during all simulations. The parameter set used for the simulations throughout this paper is given in Table I.

[1] O. Diez-Martínez and J.P. Segundo, Biol. Cybern. **47**, 33 (1983).

[2] A.M. Kunysz *et al.*, Am. J. Physiol. **273**, 331–346 (1997).

[3] J. Lewis *et al.*, Phys. Lett. A **125**, 119 (1987); L. Glass and Z. Wan-Zhen, Ann. N.Y. Acad. Sci. **591**, 316 (1990).

[4] G.W.M. Westby, J. Comp. Physiol. **96**, 307 (1975).

[5] J.M. Bekkers and C.F. Stevens, Proc. Natl. Acad. Sci. U.S.A. **88**, 7834 (1991).

[6] A.B. Karabelas and D.P. Purpura, Brain Res. **200**, 467-73 (1980).

[7] D.M. Wilson and I. Waldron, Proc. IEEE **56**, 1058 (1968).

[8] K. Pakdaman *et al.*, Neural Networks **9**, 797 (1996); Int. J. Modeling Simulation (to be published).

[9] A.L. Hodgkin and A.F. Huxley, J. Physiol. (London), **117**, 500 (1952).

[10] L. Glass and M. Mackey, *From Clocks to Chaos* (Princeton University Press, Princeton, 1988); see also references in L. Glass, Chaos **1**, 13 (1991); Stiber *et al.*, BioSystems **40**, 177 (1997).

[11] L. Glass and A.T. Winfree, Am. J. Physiol. **246**, R251 (1984).

[12] M. Kawato, J. Math. Biol. **12**, 13 (1981).

[13] R.E. Plant, SIAM J. Appl. Math. Mech. **40**, 152 (1981).

[14] J. Foss *et al.*, Phys. Rev. Lett. **76**, 708 (1996).

[15] M. Hines, in *Neural Systems: Analysis and Modeling*, edited by F. Eeckman (Kluwer, Dordrecht, 1993).